J Mater Sci (2011) 46:6801–6811
DOI 10.1007/s10853-011-5639-9

Influence of process and test parameters on the mechanical properties of flax/epoxy composites using response surface methodology

P. B. Gning · S. Liang · L. Guillaumat · W. J. Pui

Received: 4 January 2011 / Accepted: 16 May 2011 / Published online: 4 June 2011

Abstract This article presents investigations on the influence of process and test parameters on the mechanical and physical properties of flax/epoxy composites using experimental design method. Specimens fabricated and tested with parameters given by a Doehlert experimental design system have been submitted to quasi-static mechanical loadings, as well as fibre volume fraction and ply thickness measurements. Response surfaces methodology allowed the determination of empirical polynomials corresponding to mechanical responses and to fibre content measurements. The study showed the strong influence of the temperature test parameter on material's mechanical properties and specimens' fracture, followed by compression pressure and number of plies parameters.

Introduction

The interest in environmentally friendly materials is continuously increasing due to the development of a global ecological consciousness. An objective of the research world is to integrate biodegradable or recyclable reinforcement in composite materials as much as possible. Vegetal fibres are a renewable resource, fully combustible and the manufacturing process is less energy consuming than the elaboration of mineral fibres [1]. Particularly, certain bio-sourced fibres (e.g. flax, hemp…) can offer specific mechanical properties comparable to glass fibres due to their low density [2].

On the other hand, vegetal fibres present some disadvantages, which limit its industrial development for the moment. First, natural fibre properties are harvest dependent. The seed variety, soil characteristics, local weather climate, fertilizer and plant maturity can influence the fibre's chemical composition and geometry, which have effects on the mechanical properties [3, 4].

The macroscopic properties of flax/polymer laminates have been studied in [5–8]. Charlet et al. [5] identified that the longitudinal stiffness and ultimate strength of unidirectional (UD) laminates increase linearly with the fibre volume fraction and the scattering of mechanical properties of composites has trends comparable to single fibres. Nevertheless, the properties of single fibres are higher than UD reinforcements ones. Baley et al. [6] observed that untreated flax fibres/polyester UD composites submitted to transverse tensile load exhibited cracks within the matrix and at interfaces in addition to cracks through individual fibres.

Authors focussed on the improvement of interfacial adhesion of fibre/matrix systems to reduce the possibilities of crack development. Encouraging results show that alkalisation enhances fibre/matrix bonding [3, 8]. Investigations conclude that further improvements of the process (treatment times and concentrations) are needed to reach the synthetic glass/matrix adhesion level [3, 8, 9]. Tensile and flexural tests on flax/polymer composites confirmed the increase of mechanical properties due to fibre treatments [7, 8]. The effects of thermal treatments on flax/PLLA interfacial properties have been investigated by Le Duigou et al. [10]. The study revealed that low cooling kinetics increases matrix crystallization and adhesion properties [11].

P. B. Gning (✉) · S. Liang · L. Guillaumat
DRIVE–E.A. 1859, ISAT, 58027 Nevers Cedex, France
e-mail: Papa-Birame.Gning@u-bourgogne.fr

W. J. Pui
UTP, Bandar Seri Iskandar, 31750 Tronoh, Perak Darul Ridzuan, Malaysia

In this article, an experimental design analysis was used to measure the influence of the laminate number of layers, the moulding compression pressure and the temperature test on the mechanical properties and fibre volume fraction and ply thickness measurements of flax/epoxy composites. A response surface methodology (RSM) enabled the assessment of variables and the identification of their effects on measured data with a minimum of experiments [12].

Experimental design

The input variables have influence on the output characteristics simultaneously, and it is often difficult to model analytically physical systems with simple relations. RSM allows to establish empirical polynomials describing accurately the variation of measured responses in the experimental region. In particular, Doehlert [13, 14] experimental design system permits to calculate the coefficients of a second-order polynomial. The experimental points are uniformly distributed in the experimental design space, and new experimental points can be easily added whilst preserving tests already done. The mathematical form of the RSMs is described in Eq. 1 [15], in which Y stands for the selected response amongst measured data.

$$Y = b_0 + \sum_{i=1}^{k} b_i x_i + \sum_{i=1}^{k} b_{ii} x_i^2 + \sum_{i=1}^{k} \sum_{j=1}^{k} b_{ij} x_i x_j \quad (1)$$

The coded variables x_i are associated to the k input factors. b_0, b_i to b_{ij} represent the model coefficients, corresponding to the value of the centre domain's response, the first-order, the square and the coupling terms, respectively. Indeed, b_{ij} represents the interactions between two input variables, and b_{ii} corresponds to the second-order non-linearity. The manipulative factors are the composite number of layers (x_1), followed by the stacking pressure during the moulding process (x_2) and finally the climatic room temperature (x_3) during mechanical testing stage. The interval of each factor is given in Table 1. The variables are expressed in centred and reduced co-ordinates. They are normalized according to the interval within $[-1, +1]$, which represents the minimum and maximum levels, respectively. The chosen centre of the region corresponds to 6 plies, 4.5 bars and 70 °C. The physical boundaries are 2–10 for number of plies, 2–7 bars for the stacking pressure during the process and 8.7–131.3 °C for the testing temperature values.

$$N = k^2 + k + 1 \quad (2)$$

The Doehlert design system for three factors ($k = 3$) consists of 13 experiments to cover the spherical domain [12]. The number of experiments (N) is calculated by Eq. 2. The codification of the experiments is detailed in Table 2. In fact, x_1 parameter has an even number of plies following symmetric layers arrangement to avoid tension-bending coupling stresses. Depending on x_3 coefficients, the range of temperature test is from 20 to 120 °C corresponding to coded limits $[-0.816, 0.816]$. The responses investigated are the mechanical properties carried from both tensile and in-plane shear testing and the fibre volume fraction and ply thickness measurements.

Experimental methods

Material

A commercial dry roller of flax ordered from local textile company CRST is used to fabricate the specimens of the above test matrix (Table 2). The flax is of the Hermès variety cultivated in northern France. Flax stems were retted and stripped to extract fibres, then hackled without being twisted and aligned to produce single UD layer. Fibres were not submitted to chemical treatment. The bidirectional non-crimp fabric is made of two perpendicular identical UD layers stitched together using a cotton thread. The cotton's areal weight is 2 g/m^2, and the distance between two parallel stitch lines is 10 mm. The average areal weight of the double ply (m_{fs}) is 237 g/m^2. The epoxy matrix used is a mixture of SR 8200 resin and SD 8205 hardener supplied by SICOMIN company, having a density (ρ_m) of 1140 kg/m^3.

Based on Table 2 experiments, layers were cut from the roller and were manually impregnated with the liquid resin, before being stacked in steel rigid moulds and compressed between the two heating plates of the ENERPAC compression-moulding machine. The compression machine is equipped with a hydraulic cylinder that ensures the compression pressure. The polymerization cycle starts by a heating slope of 2 °C/min until 60 °C followed by a constant temperature stage of 1 h under the specified monitored pressure and then finishes by air cooling step.

Table 1 Experimental domain for the three studied factors

Coded levels and physical values

Factors	Variables	Level (−1)	Level (0)	Level (1)
Number of plies	x_1	2	6	10
Stacking pressure (bar)	x_2	2.0	4.5	7.0
Temperature test (°C)	x_3	8.7	70.0	131.3

Table 2 Doehlert test matrix

Test #	Number of plies		Stacking pressure (bar)		Temperature test (°C)	
	Coded	Physical	Coded	Physical	Coded	Physical
1	0	6	0	4.5	0	70
2	1	10	0	4.5	0	70
3	−1	2	0	4.5	0	70
4	0.5	8	0.866	6.7	0	70
5	−0.5	4	−0.866	2.3	0	70
6	0.5	8	−0.866	2.3	0	70
7	−0.5	4	0.866	6.7	0	70
8	0.5	8	0.289	5.2	0.816	120
9	−0.5	4	−0.289	3.8	−0.816	20
10	0.5	8	−0.289	3.8	−0.816	20
11	0	6	0.577	5.9	−0.816	20
12	−0.5	4	0.289	5.2	0.816	120
13	0	6	−0.577	3.1	0.816	120

Coded coefficients and corresponding natural variables

The evolution of the modulus and the damping of the matrix cured in the same conditions than the samples were determined with a dynamic mechanical analyser (VA4000-Metravib) over a temperature range from 20 to 120 °C (Fig. 1). Temperature scanning from low to high was performed with a heating rate of 1 °C/min at a tensile testing frequency of 1 Hz. The glass transition temperature (T_g) corresponding to the peak tan δ is 87 °C, and the elastic modulus evolution of the matrix appears linear from 20 °C to T_g. The value of T_g is lower than the upper bond of the range of temperature test (20–120 °C) because the objective of this exploratory work is to investigate the mechanical behaviour of flax/epoxy composites below and above the matrix T_g. The void fraction is not measured, but seems to be acceptable according to observations.

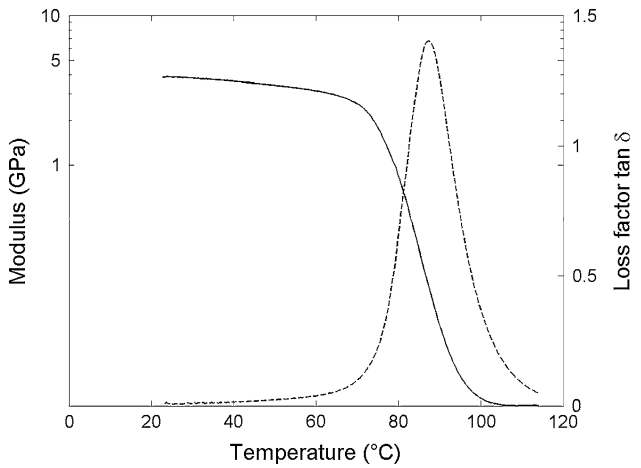

Fig. 1 Matrix's storage modulus and loss factor tan δ as a function of temperature for a testing frequency of 1 Hz

Tensile and in-plane shear testing

Two sets of 13 plates are fabricated, in agreement with the experimental design in Table 2. Uniaxial tensile and in-plane shear specimens were cut from plates to nominal dimensions of 250 × 25 mm using a 3000 rpm abrasive disc (Fig. 2) [16, 17]. x and y axes are designated as the loading and the in-plane perpendicular direction, respectively. Tensile and shear specimens have [0, 90] and [45, −45] symmetric lay-ups. The thicknesses of specimens (t) depend on the number of layers (n) and the process compression pressure parameters of the test matrix. No lubrication fluid is used during cutting to avoid moisture absorption. Cut edges were lightly polished with fine sandpaper. After abrasion of the end surfaces, soft aluminium end tabs of 50 × 25-mm and 3-mm thick were glued on with Huntsman Araldite epoxy-resin paste and cured in a dry oven at 40 °C for 2 h. One strain gauges rosette (Kyowa) with two perpendicular elements of 5-mm long and 5% maximum strain each is adhesively bonded to the centre of one side of the specimen. The gauges elements are oriented parallel and perpendicular to the loading

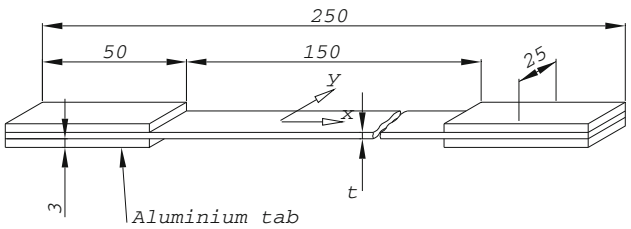

Fig. 2 Geometry of tensile and in-plane shear specimens. Notations with coordinates system. Units in mm

direction. For testing, the specimens are clamped at the end tabs between the grips of a MTS 809 testing machine. The specimen and machine grips are stationed inside a Servathin climatic chamber with constant temperature heating for 1 h before test commencement.

Longitudinal modulus (E_x), ultimate tensile strength (X_x), failure tensile strain ($\varepsilon_x^{\max}$) and Poisson's ratio (v_{xy}) are determined from the tensile tests. Because of the lay-up symmetry, longitudinal and transversal data are considered equivalent. Shear modulus (G_{xy}), strength (S_{xy}) and failure strain ($\varepsilon_{xy}^{\max}$) are measured from the shear tests. The in-plane shear test consists of a tensile loading of specimen with fibre aligned at ±45° with respect to the loading direction. The shear strain corresponds to the difference between the recorded strain signals by two gauges. S_{xy} is the maximum stress before specimen failure or the stress corresponding to 5% strain at the end of test [17]. All tests are performed at a constant 2 mm/min crosshead speed rate. The experimental measurements are recorded by an ES1M data acquisition system with 10 Hz quasi-static frequency.

Fibre volume fraction and ply thickness measurement

$$\rho_f = \frac{m_{fs} \cdot n}{t - \frac{m_{sp}/a_{sp} - m_{fs} \cdot n}{\rho_m}} \quad (3)$$

$$V_f = 1 - \frac{m_{sp} - m_{fs} \cdot a_{sp} \cdot n}{\rho_m \cdot a_{sp} \cdot t} \quad (4)$$

It is of concern in this study to analyze the influence of the applied compression pressure during the fabrication and the number of layers (n) on the fibre volume fraction (V_f) and layer thickness (t_{layer}) of the composite plates. t_{layer} is the thickness of the plate (t) divided by its number of layers (n). Four square-shaped specimens of 30 mm side length are cut-out randomly from each fabricated for thickness, area (a_{sp}) and mass (m_{sp}) measurements. The flax layer density calculated using Eq. 3 is 1498 kg/m^3 with a coefficient of variation of 2.8%. ρ_m represents the matrix density. This result is coherent with flax density of 1530 kg/m^3 published by Ganster [18]. Then, the fibre volume fractions of the plates are calculated using Eq. 4.

SEM micrographs of specimens' cross-sectional surfaces show the presence of a superficial resin coat of 0.1-mm thick on average on the top and bottom surfaces of the plate (Fig. 3). This resin layer makes the ply distribution non-homogeneous throughout the whole thickness. For example, both composite plates of 2 and 10 double-plies, with the same compression pressure, have the same thickness of matrix coat. In order to have more accurate data on fibre fraction and ply thickness measurements, the thickness of this superficial resin coat has to be considered in the specimen thickness (t) determination. The tests results are detailed subsequently.

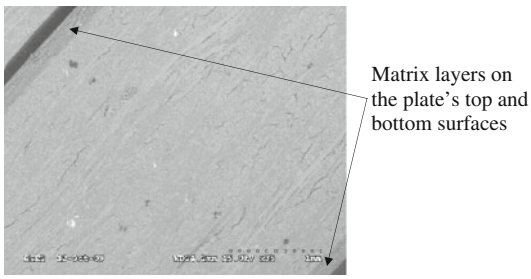

Fig. 3 Macrograph illustrating the superficial resin coat on specimen with 6 plies and 6.7 bars compression pressure

Results and discussion

The influence of process and test parameters on the mechanical and physical properties is described in this section. The measured tensile properties (longitudinal modulus, ultimate tensile strength, failure strain and Poisson's ratio), in-plane shear properties (shear modulus, ultimate strength and failure strain), fibre volume fraction and ply thickness measurements are given in Table 3. The thirteen test conditions of the experimental design matrix were repeated at least three times to measure the data scattering. RS of the experimental design is built based on these results.

Mechanical tests

From Table 3, it is remarkable that the testing temperature has the highest influence on material's mechanical properties amongst the three varying parameters. For instance, when data are sorted according to the test temperature, we can observe the important overall decrease of the stiffness with the rise of the temperature followed by a moderation in the drop, as shown in Figs. 4a and 5a. On average, the decrease of tensile and shear modulus is of 6.5 and 1.3 GPa, between 20 and 70 °C, then of 1 and 0.5 GPa between 70 and 120 °C, respectively. The decrease of modulus trends at lower temperatures is about seven and three times higher than at higher temperatures. This remark is particularly important because it implies that temperature has to be controlled for flax/epoxy composites testing. As for the compression pressure factor, the data show a wavy aspect (Figs. 4b and 5b). No clear trend is noticeable when data are sorted according to the number of plies parameter. The actual influence of each parameter will be determined in the experimental design analysis stage.

The plot of typical quasi-static stress–strain responses can highlight manipulative factors' influence on mechanical behaviour. Therefore, two to three curves of tested specimens subjected to tensile and in-plane shear loadings are plotted in Figs. 6, 7 and 8. The graphs compare,

Table 3 Elastic and failure responses of quasi-static tensile and in-plane shear tests with fibre fraction and ply thickness measurements

Test #	Specimen type	E_x (GPa)	X_x (MPa)	ε_x^{max} (%)	ν_{xy}	G_{xy} (GPa)	S_{xy} (MPa)	ε_{xy}^{max} (%)	V_f (%)	t_{layer} (mm)
1	[6 plies; 4.5 bars; 70 °C]	8.52 (2.75)	96.0 (16.8)	1.33 (0.22)	0.087 (0.07)	0.74 (0.09)	20.9 (0.8)	>10	39.5 (2.3)	0.40 (0.017)
2	[10 plies; 4.5 bars; 70 °C]	6.66 (0.37)	90.1 (8.4)	1.6 (0.4)	0.21 (0.04)	1.07 (0.15)	21.0 (2.8)	>10	40.1 (0.9)	0.40 (0.009)
3	[2 plies; 4.5 bars; 70 °C]	6.72 (0.15)	76.5 (8.1)	1.1 (0.1)	0.16 (0.09)	0.73 (0.07)	19.1 (1.3)	>10	37.1 (1.1)	0.42 (0.010)
4	[8 plies; 6.7 bars; 70 °C]	8.01 (0.10)	99.2 (7.0)	1.33 (0.24)	0.094(0.043)	1.04 (0.19)	24.1 (1.2)	>10	43.1 (0.8)	0.36 (0.005)
5	[4 plies; 2.3 bars; 70 °C]	7.24 (0.68)	90.8 (3.2)	1.3 (0.13)	0. 119 (0.010)	0.75 (0.08)	19.0 (0.6)	>10	35.2 (0.6)	0.44 (0.003)
6	[8 plies; 2.3 bars; 70 °C]	6.69 (0.46)	96.8 (3.2)	1.3 (0.1)	0.11 (0.03)	0.70 (0.07)	18.2 (1.1)	>10	36.3 (0.6)	0.43 (0.004)
7	[4 plies; 6.7 bars; 70 °C]	8.73 (0.52)	99.5 (16.3)	1.13 (0.17)	0.115 (0.060)	0.90 (0.16)	19.8 (1.0)	>10	40.8 (1.3)	0.38 (0.010)
8	[8 plies; 5.2 bars; 120 °C]	6.50 (0.65)	54.8 (12.4)	0.92 (0.14)	0.200 (0.021)	0.32 (0.02)	7.8 (1.2)	3.4 (0.3)	40.5 (0.6)	0.39 (0.006)
9	[4 plies; 3.8 bars; 20 °C]	12.74 (0.91)	130.0 (5.4)	1.3 (0.1)	0.12 (0.04)	2.10 (0.09)	37.9 (1.5)	3.8 (0.9)	37.2 (0.4)	0.41 (0.003)
10	[8 plies; 3.8 bars; 20 °C]	12.98 (1.31)	148.1 (19.3)	1.44 (0.23)	0.108 (0.020)	2.07 (0.06)	45.6 (1.9)	4.7 (0.1)	37.7 (0.5)	0.41 (0.003)
11	[6 plies; 5.9 bars; 20 °C]	15.61 (0.38)	150.0 (10.7)	1.3 (0.1)	0.13 (0.02)	2.34 (0.17)	43.5 (1.3)	4.0 (0.8)	42.0 (0.8)	0.38 (0.005)
12	[4 plies; 5.2 bars; 120 °C]	6.34 (0.76)	61.9 (4.0)	0.94 (0.09)	0.097 (0.028)	0.36 (0.05)	8.18 (0.4)	3.1 (0.2)	40.2 (2.1)	0.39 (0.017)
13	[6 plies; 3.1 bars; 120 °C]	6.33 (0.85)	58.3 (6.5)	0.92 (0.12)	0.177 (0.102)	0.30 (0.03)	7.8 (0.2)	3.0 (0.5)	37.1 (1.1)	0.44 (0.009)

Average values and standard deviations in brackets

respectively, experiments with different number of plies, compression pressures and temperatures. First, the global behaviour of samples seems linear during uniaxial tension without activation of nonlinear effects. The load keeps on increasing up to a peak value followed by a brittle failure, and then the force drops drastically to zero. On the other hand, in-plane shear responses present similar features in the first part of the curves, followed by the development of a non-linear stage. Test results of specimens having 2, 6 and 10 layers with 4.5 bar compression pressure and 70 °C temperature test are plotted in Fig. 6a, b. Tensile and shear curves present similar trends and measured data are close, as noticeable in Table 3. This remark suggests that the influence of the number of plies parameter does not have a significant enough effect. The influence of laminates' stacking pressure can be analyzed through the behaviour of two specimen types, e.g. [8 plies, 2.3 bars, 70 °C] and [8 plies, 6.7 bars, 70 °C] given in Fig. 7a, b. Tensile plots seems very close compared to in-plane shear ones. Nevertheless, related experimental data tabulated in Table 3 reveal a slight influence of the stacking pressure on laminates mechanical properties, even if it is not a preponderant parameter. Finally, typical specimen types' responses of [6 plies, 5.9 bars, 20 °C], [6 plies, 4.5 bars, 70 °C] and [6 plies, 3.1 bars, 120 °C] are presented in Fig. 8a, b. It appears that specimens tested at room temperature present the higher experimental levels than at 70 and 120 °C. Besides, as the influence of specimen number of plies and compression pressure are considered weak, the differences noted between curves are mainly attributable to climatic room temperature effect. Indeed, all elastic and failure material properties, with the exception of shear failure strain data at 70 °C, decrease significantly with temperature test conditions, followed by stacking pressure and the number of plies factors (Table 3).

The observation of specimens' fracture modes reveal clearly that the failure is mainly influenced by the test temperature parameter, regardless of other parameter change, both in tensile or in-plane shear testing. Two main modes are identified in uniaxial tensile tests. At 20 and 70 °C, the specimens' fracture is brittle. The reinforcement breakage occurs at one local place, in the current area of the specimen, perpendicularly to the loading direction. Figure 9a, b shows the fracture aspect of a [4 plies, 3.8 bars, 20 °C] and [8 plies, 2.3 bars, 70 °C] specimens under tension. At 120 °C, the main (notable) fracture mode is interlaminar delamination. Indeed, at a high temperature, the softening of the epoxy matrix causes the weakening of the cohesion between the 0/90° double layers, thus the peeling stresses resulting from the loading of the cross-ply laminate initiate debonding at the interface of adjacent plies. Figure 9c presents the photographs of a fractured [8 plies, 5.2 bars, 120 °C] specimen submitted to tensile

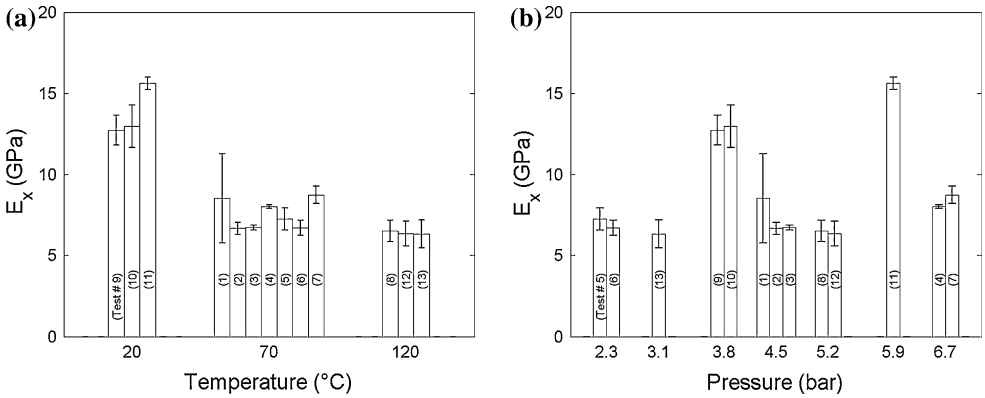

Fig. 4 Graphs of tensile modulus as a function of temperature test (**a**) and compression pressure (**b**). Experiment number of test matrix

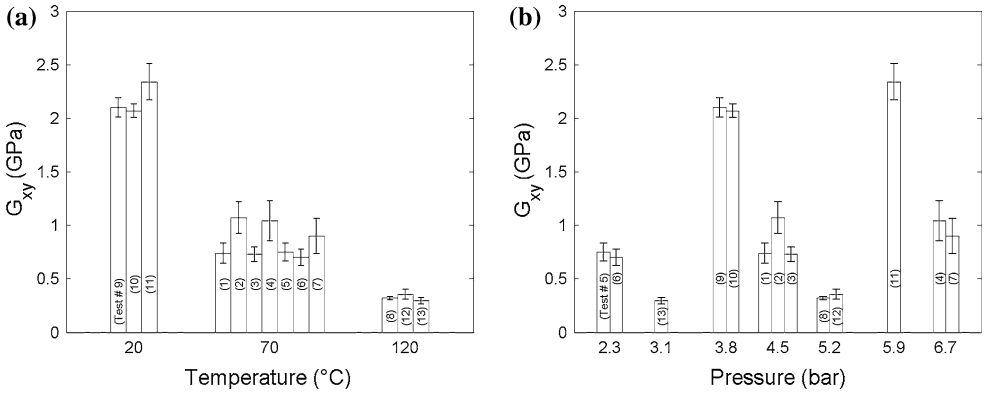

Fig. 5 Graphs of shear modulus as a function of temperature test (**a**) and compression pressure (**b**)

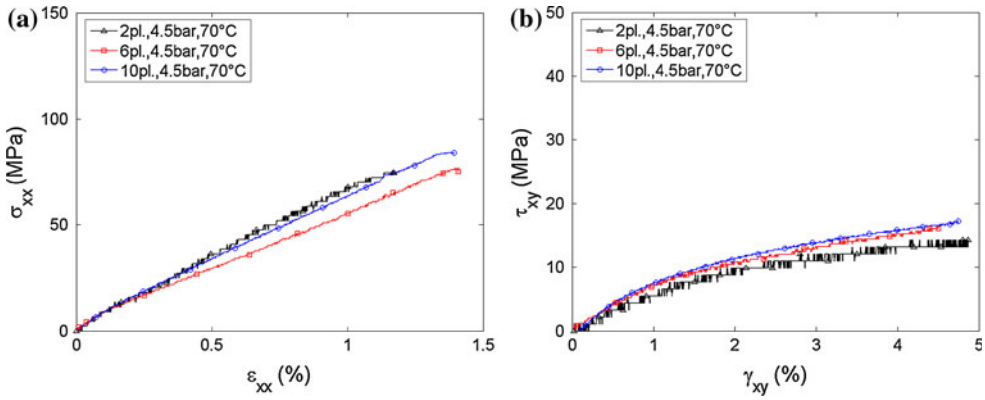

Fig. 6 Typical stress–strain curves of specimens under tensile (**a**) and shear loading (**b**): [2 plies, 4.5 bars, 70 °C], [6 plies, 4.5 bars, 70 °C] and [10 plies, 4.5 bars, 70 °C]

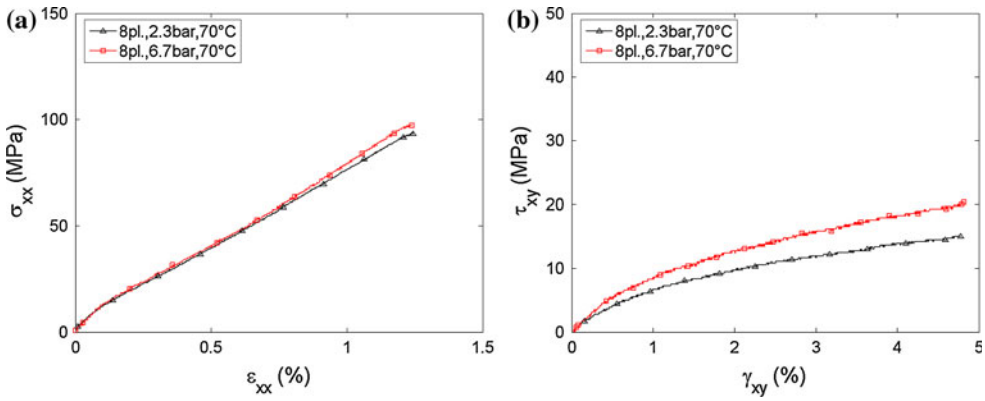

Fig. 7 Typical stress–strain curves of specimens under tensile (**a**) and shear loading (**b**): [8 plies, 2.3 bars, 70 °C] and [8 plies, 6.7 bars, 70 °C]

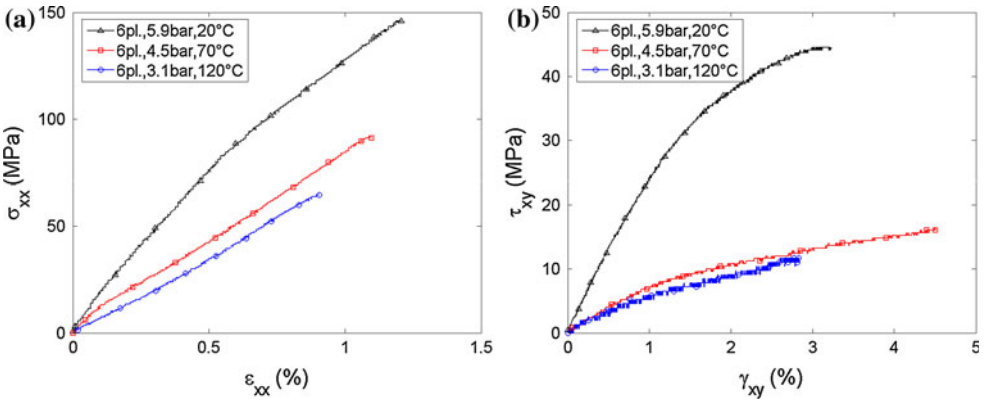

Fig. 8 Typical stress–strain curves of specimens under tensile (**a**) and shear loading (**b**): [6 plies, 5.9 bars, 20 °C], [6 plies, 4.5 bars, 70 °C] and [6 plies, 3.1 bars, 120 °C]

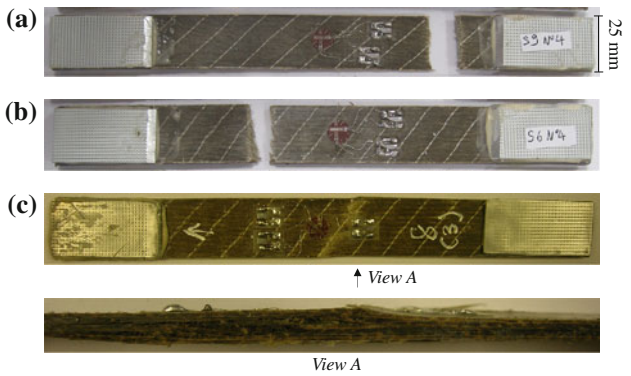

Fig. 9 Micrographs of fractured specimens [4 plies, 3.8 bars, 20 °C] (**a**), [8 plies, 2.3 bars, 70 °C] (**b**) and [8 plies, 5.2 bars, 120 °C] (**c**) under tensile loading

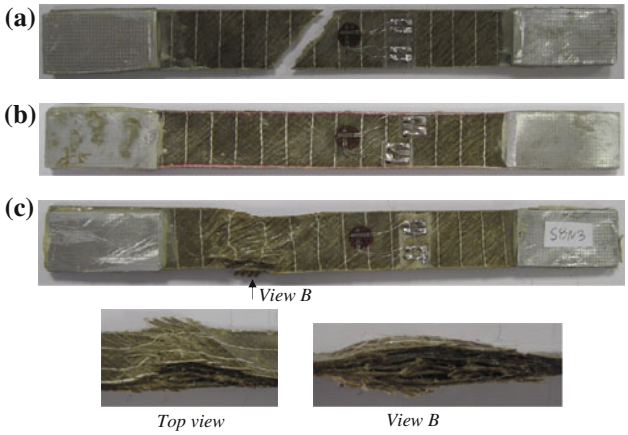

Fig. 10 Micrographs of fractured specimens [4 plies, 3.8 bars, 20 °C] (**a**), [8 plies, 2.3 bars, 70 °C] (**b**) and [8 plies, 5.2 bars, 120 °C] (**c**) under in-plane shear loading

loading. As for in-plane shear test, three typical modes are noticed. The specimen's fracture at 20 °C is sudden, in spite of the fracture phenomenology differs from tensile specimen one. The crack propagates across the sample from one free-edge to another. The fracture results from the concomitancy of intra-laminar fibre/matrix debonding and fibre breakage with an angle of 45°. Because of this combination of modes, the crack path is not regular and straight, but the fracture (line) morphology presents 'saw-tooth' shape. Figure 10a exhibits a [4 plies, 3.8 bars, 20 °C] fractured specimen under in-plane shear loading. Conversely, no specimen breakage is noticed at 70 °C. The samples elongate up to important strain levels, higher than gauge capacity recording without failure. Moreover, the estimated reached shear strain after the test stop is likely to surpass 10% (Fig. 10b [8 plies, 2.3 bars, 70 °C]). Failure phenomenology is similar to uniaxial tensile case at 120 °C. The softening of the matrix is important, and then cross-ply debonding occurs followed by the re-alignment of ±45° fibres. The failure mode is a successive combination of through the thickness delamination and in-plane fibre/matrix debonding as illustrated in Fig. 10c for a [8 plies, 5.2 bars, 120 °C] tested specimen.

Parameters' influence

The experimental design technique is used to determine as precisely as possible the effects of the manipulative parameters on mechanical responses (tensile and shear measured data) extracted from Table 3. Ten model coefficients (Eq. 2) of empirical polynomials' (b_0 to $b_{2\text{-}3}$) of x_1, x_2 and x_3 factors are given in Table 4. The experimental results are computed by Nemrodw® software [19].

Calculated model coefficient b_0 for all responses correspond to the experimental results at the centre of the domain of study, i.e. [6 plies, 4.5 bars, 70 °C] data in Table 3. As for the other coefficients, and apart from the Poisson's ratio response, stiffness, ultimate strengths and failure strains responses of both tensile and shear loading tests are led by overall temperature coefficients, i.e. b_3 and $b_{3\text{-}3}$, whose coefficients' absolute values are the highest ones. It appears clearly that these responses are largely sensitive to temperature parameter and squared temperature parameter. Besides, some coupling effects between parameters are also noticeable. Differently, $b_{1\text{-}1}$ referring to number of plies parameter, presents the

Table 4 Model coefficients for all RSs polynomials

Coefficients	Responses								
	Y_1 (GPa)	Y_2 (MPa)	Y_3 (%)	Y_4	Y_5 (GPa)	Y_6 (MPa)	Y_7 (%)	Y_8 (%)	Y_9 (mm)
b_0	8.52	96.00	1.33	0.087	0.74	20.92	10.00	39.36	0.40
b_1	−0.12	5.47	0.18	0.020	0.09	1.83	0.16	1.27	−0.01
b_2	1.01	3.94	−0.04	−0.006	0.15	1.75	−0.01	3.81	−0.04
b_3	−4.51	−51.46	−0.26	0.024	−1.13	−21.07	−0.63		
$b_{1\text{-}1}$	−1.83	−12.71	0.03	0.098	0.16	−0.84	−0.00	−0.90	0.01
$b_{2\text{-}2}$	−0.51	4.85	−0.09	−0.003	0.09	−0.55	−0.00	−0.34	0.00
$b_{3\text{-}3}$	2.90	8.74	−0.28	0.053	0.70	6.67	−9.52		
$b_{1\text{-}2}$	−0.10	−3.60	0.10	−0.007	0.11	2.96	−0.00	0.53	−0.01
$b_{1\text{-}3}$	−0.02	−14.14	−0.13	0.072	−0.05	−5.98	−0.38		
$b_{2\text{-}3}$	−1.44	−1.64	0.02	−0.069	−0.18	−0.99	0.37		

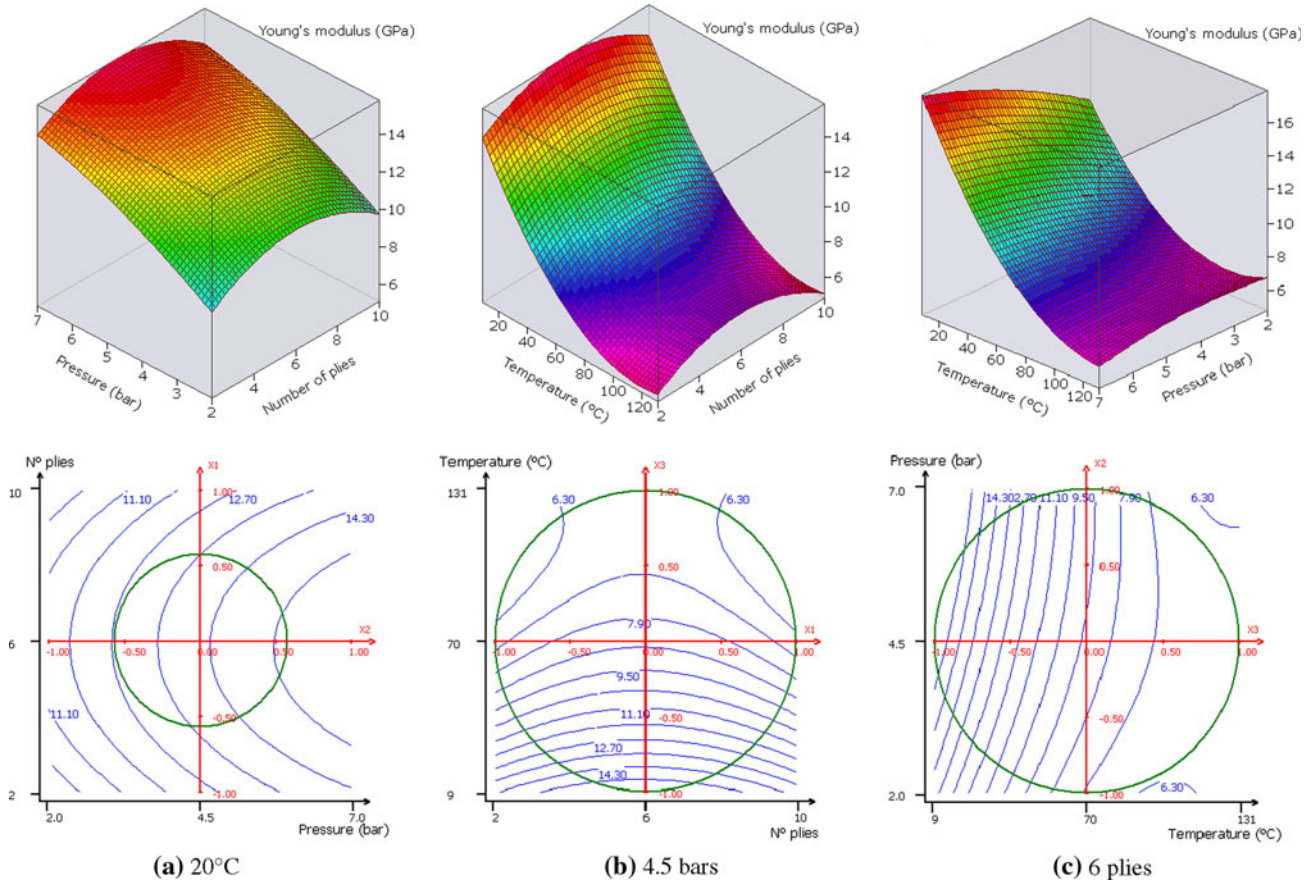

Fig. 11 Response surface graphs and contour plots of longitudinal modulus as a function of test factors

equivalent weight than temperature parameter, in Poisson's ratio response. In fact, v_{xy} is calculated as the absolute value of transversal and longitudinal strains ratio. So, for this balanced cross-ply laminate, because fibres are stiffer and less sensitive to temperature than the epoxy matrix [20], the ratio of strains is influenced by the amount of reinforcement depending on the number of layers.

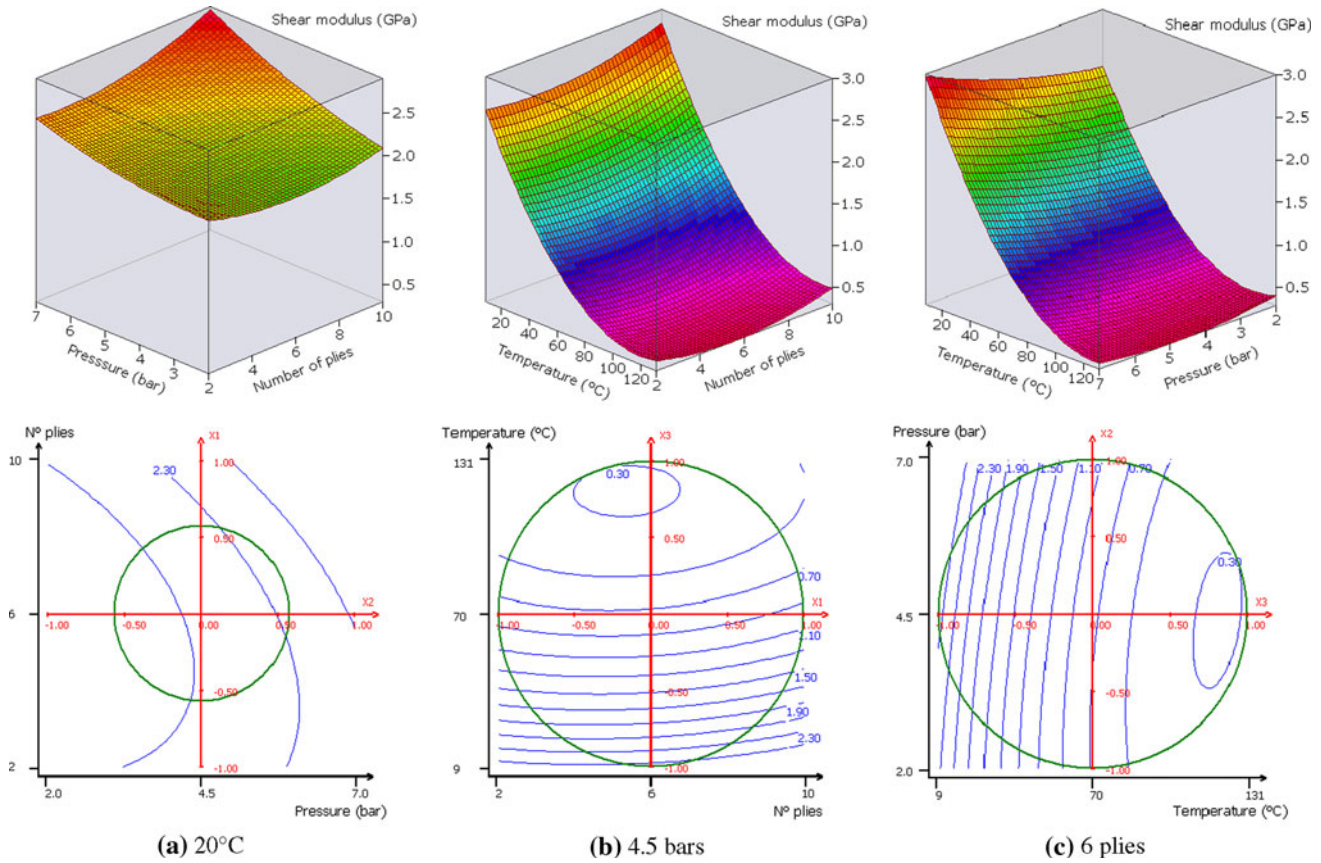

Fig. 12 Response surface graphs and contour plots of shear modulus as a function of test factors

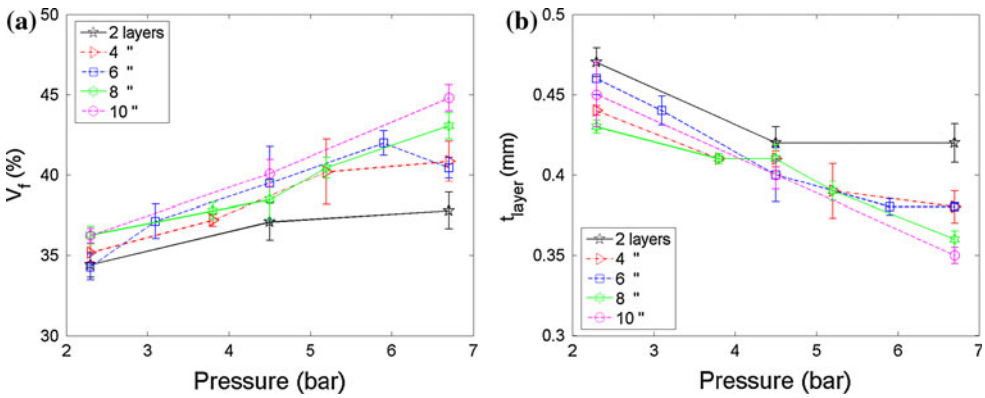

Fig. 13 Fibre volume fraction (**a**) and layer thickness (**b**) as a function of compression pressure

$$Y_1 = 8.52 - 0.12x_1 + 1.01x_2 - 4.51x_3 - 1.83x_1^2 - 0.51x_2^2 + 2.90x_3^2 - 0.10x_1x_2 - 0.02x_1x_3 - 1.44x_2x_3 \quad (5)$$

$$Y_5 = 0.74 - 0.09x_1 + 0.15x_2 - 1.13x_3 + 0.16x_1^2 + 0.09x_2^2 + 0.70x_3^2 + 0.11x_1x_2 - 0.05x_1x_3 - 0.18x_2x_3 \quad (6)$$

Response surfaces are plotted for two of the factors, whilst the third one is fixed at a specified level. As tensile and shear responses show the same trends in the studied experimental domain, RS graphs and contour plots of tensile (Y_1) and shear (Y_5) modulus are given as examples in Figs. 11 and 12, based on Eqs. 5 and 6. The b_{ij} coefficients are reported in Table 4. Temperature appears as the most influencing parameter in Fig. 11b and c as well as in Fig. 12b, c. One can notice that, for a fixed temperature at 20 °C, contour plots of E_x and G_{xy} are continuously increasing with the fabrication pressure parameter (Figs. 11a and 12a). Overall, the same phenomenon is noticed for all other experimental responses.

Besides, in order to determine which of number of plies or compression pressure parameter has the greater

influence, fibre fraction and ply thickness have been measured (Table 3). According to the rule of mixture equations, the increase of fibre content has direct influence on laminate's mechanical properties [11]. Figure 13a, b represents plots of the trends of fibre fraction and ply thickness measurements as a function of compression process pressure. In spite of the scatter in Fig. 13a, we can observe the general increase of the fibre fraction from 34 to 46% with the compression pressure ranging from 2 to 7 bars in conformity with the experimental design bounds (Table 1). The plots also reveal that for a given pressure, V_f is increasing with n parameter. This means that the more layers the plate has, the higher the fibre fraction is. Inversely, the ply thickness decreases with the pressure increase from 0.48 to 0.36 mm (Fig. 13b). The trends confirm the influence of the number of plies or plate thickness on the layer thickness. Further investigation is needed to confirm what appears to be a lay-up or plate thickness effect and to determine the physical limits of fibre fraction and ply thickness data for higher compaction levels (>7 bars) during the process.

$$Y_8 = 39.36 + 1.27x_1 + 3.81x_2 - 0.90x_1^2 - 0.34x_2^2 + 0.53x_1x_2 \quad (7)$$

$$Y_9 = 0.402 - 0.009x_1 - 0.040x_2 + 0.006x_1^2 + 0.001x_2^2 - 0.005x_1x_2 \quad (8)$$

A Doehlert design system is used to evaluate the influence of number of plies (x_1) and compression pressure (x_2) parameters on laminates' fibre fraction and ply thickness. For two parameters ($k = 2$), only experimental results from number 1 to 7 in Table 3 are required to establish the second-order polynomials (Eq. 2). Moreover, the remaining experimental results are used to enrich the empirical model for more accuracy in V_f and t_{layer} coefficients, filled in Table 4. The corresponding polynomials Y_8 and Y_9 are given by Eqs. 7 and 8.

RS plotted in Fig. 14a, b reveals that compression pressure has more influence over the number of plies parameter on the fibre content and ply thickness. This implies a greater presence of reinforcement in specimens leading to higher mechanical behaviour. So, as the number of plies parameter has a smaller influence on fibre volume fraction, its effect on mechanical properties is consequently minor. Finally, the laminate's number of plies appears to have the weakest influence amongst the three manipulative variables.

Conclusions

This article presents the influence of process and test parameters on the mechanical and physical properties of flax/epoxy composites. Test parameters are established using a Doehlert design system. The three factors considered are composite number of plies, the stacking pressure during the curing process and the room temperature during uniaxial tensile and in-plane shear test. Factors' coefficients are given by the design codification. Specimens are made by hand lay-up process of double cross-plies of dry flax impregnated with an epoxy matrix. Fibres are aligned parallel and perpendicular to the grip-to-grip direction for uniaxial tensile specimens and oriented at ±45° with the loading axis. Thirteen sets of tensile, shear and fibre content specimens are fabricated and tested based on the test matrix.

For tensile samples, the fracture consisted of brittle failure up to 70 °C. As for shear samples, the breakage is sudden, and the fracture morphology presents a 'sawtooth' shape at low temperature. At 70 °C, important elongation

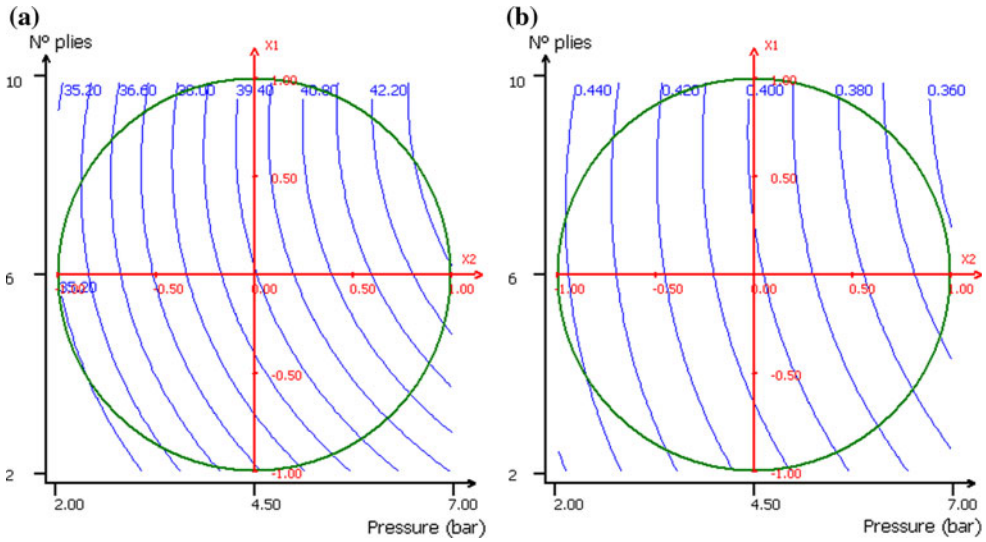

Fig. 14 Contour plots of fibre volume fraction (**a**) and relative ply thickness (**b**) variation as a function of number of plies and stacking process pressure factors

is noticed without breakage. For both specimen types, interlaminar debonding at interfaces of adjacent double-plies due to matrix softening happened at high temperature. The polynomials' coefficients of all response surfaces were calculated. The study showed analytically that the temperature test is the most influential parameter on tensile and shear mechanical properties. Second RS analysis revealed the strong dependence of fibre fraction and ply thickness on the compression pressure parameter and on the number of plies factors to a lesser extent. The fibre content, therefore, has a direct effect on mechanical properties.

Acknowledgements The financial support of the Faber fund from the Bourgogne Region, France is gratefully acknowledged.

References

1. Corbière-Nicollier T, Gfeller Laban B, Lundquist L, Leterrier Y, Månson JAE, Jolliet O (2001) Resour Conserv Recycl 33:267
2. Bodros E, Pillin I, Montrelay N, Baley C (2007) Compos Sci Technol 67:462
3. Baley C, Busnel F, Grohens Y, Sire O (2006) Composites A 37:1626
4. Charlet K, Jernot JP, Gomina M, Bréard J, Morvan C, Baley C (2009) Compos Sci Technol 69:1399
5. Charlet K, Baley C, Morvan C, Jernot JP, Gomina M, Bréard J (2007) Composites A 38:1912
6. Baley C, Perrot Y, Busnel F, Guezenoc H, Davies P (2006) Mater Lett 60:2984
7. Van de Velde K, Kielens P (2003) Compos Struct 62:443
8. Van de Weyenberg I, Chi truong T, Vangrimde B, Verpoest I (2006) Composites A 37:1368
9. Joffe R, Andersons J, Wallström L (2003) Composites A 34:603
10. Le Duigou A, Davies P, Baley C (2010) Compos Sci Technol 70:231
11. Zafeiropoulos NE, Baillie CA, Matthews FL (2001) Composites A 32(3–4):525
12. Guillaumat L (2000) Compos Struct 76:163
13. Doehlert DH (1970) Appl Stat 19:231
14. Doehlert DH, Klee VL (1972) Discret Math 2:309
15. Mathieu D, Phan-Tan-Luu R, Sergent M (1989) Méthodologie de la recherche expérimentale. LPRAI, Marseille
16. EN ISO 527-4 (1997) Determination of tensile properties—test conditions for isotropic and orthotropic fibre-reinforced plastic composites, July 1997
17. EN ISO 14129 (1998) Fibre-reinforced plastic composites—Determination of the in-plane shear stress/shear strain response, including the in-plane shear modulus and strength, by the $\pm$ 45° tension test method, April 1998
18. Ganster J, Fink HP (1999) Physical constants of cellulose. In: Brandup J, Immergut EH, Grulke EA (eds) Polymer handbook. Wiley, New York
19. Software Nemrodw® V 2000, LPRAI, Marseille
20. Gay D, Hoa SV, Tsai SW (2003) Composite materials design and applications. CRC Press LLC. ISBN 1-58716-084-6